Positive Heat Capacity Change upon Specific Binding of Translation Initiation Factor eIF4E to mRNA 5′ Cap[†]

Anna Niedzwiecka,[‡] Janusz Stepinski,[‡] Edward Darzynkiewicz,[‡] Nahum Sonenberg,[§] and Ryszard Stolarski*,[‡]

Department of Biophysics, Institute of Experimental Physics, Warsaw University, 02-089 Warszawa, Poland, and Department of Biochemistry and McGill Cancer Center, McGill University, Montreal, Quebec, H3G 1Y6, Canada

ABSTRACT: Specific recognition of the mRNA 5′ cap by eukaryotic initiation factor eIF4E is a rate-limiting step in the translation initiation. Fluorescence spectroscopy and high-sensitivity isothermal titration calorimetry were used to examine the thermodynamics of eIF4E binding to a cap-analogue, 7-methylGpppG. A van't Hoff plot revealed nonlinearity characterized by an unexpected, large positive molar heat capacity change ($\Delta C_p^\circ = +1.92 \pm 0.93$ kJ·mol^{-1}·K^{-1}), which was confirmed by direct ITC measurements ($\Delta C_p^\circ = +1.941 \pm 0.059$ kJ·mol^{-1}·K^{-1}). This unique result appears to come from an extensive additional hydration upon binding and charge-related interactions within the binding site. As a consequence of the positive ΔC_p°, the nature of the thermodynamic driving force changes with increasing temperature, from enthalpy-driven and entropy-opposed, through enthalpy- and entropy-driven in the range of biological temperatures, into entropy-driven and enthalpy-opposed. Comparison of the van't Hoff and calorimetric enthalpy values provided proof for the ligand protonation at N(1) upon binding, which is required for tight stabilization of the cap−eIF4E complex. Intramolecular self-stacking of the dinucleotide cap-analogue was analyzed to reveal the influence of this coupled process on the thermodynamic parameters of the eIF4E−mRNA 5′ cap interaction. The temperature-dependent change in the conformation of 7-methylGpppG shifts significantly the intrinsic $\Delta H_0^\circ = -72.9 \pm 4.2$ kJ·mol^{-1} and $\Delta S_0^\circ = -116 \pm 58$ J·mol^{-1}·K^{-1} of binding to the less negative resultant values, by $\Delta H_{sst}^\circ = +9.76 \pm 1.15$ kJ·mol^{-1} and $\Delta S_{sst}^\circ = +24.8 \pm 2.1$ J·mol^{-1}·K^{-1} (at 293 K), while the corresponding $\Delta C_{p_{sst}}^\circ = -0.0743 \pm 0.0083$ kJ·mol^{-1}·K^{-1} is negligible in comparison with the total ΔC_p°.

Cap-dependent translation of messenger RNAs in eukaryotes begins with specific recognition of the mRNA 5′ cap structure, 7-methylG(5′)ppp(5′)N (where N is any nucleotide), by the highly conserved eukaryotic initiation factor 4E (eIF4E)[1] (1). Crystal structures of murine eIF4E bound to the cap-analogues 7-methylGDP (2) and 7-methylGpppG (3) revealed specific interactions in the complex. 7-Methylguanine binding occurs via sandwich stacking between Trp102 and Trp56, and three Watson−Crick-like hydrogen bonds. The latter involve N²H, N(1)H, and O⁶ of 7-methylguanine, bound to the carboxyl group of Glu103 and the NH of the backbone of Trp102. The complex is additionally stabilized by salt bridges and direct or water-mediated hydrogen bonds between the phosphates of the cap and the side chains of Arg112, Lys162, Arg157, and Lys206, and the NH of the Trp102 and Trp166 indole rings (PDB accession numbers 1EJ1, 1L8B).

To build a biophysical basis of the 5′ cap-dependent translation initiation step and explain some discrepancies among structural, biochemical, and biological observations (2, 4−6), the crystallographic approach must be completed by thermodynamic analysis, based on spectroscopic and/or calorimetric measurements. Our previous stopped-flow and equilibrium studies together with Brownian molecular dynamics simulations showed an important role of electrostatic steering of the ligand toward the binding center of eIF4E (3, 7). Detailed binding studies enabled us to parse the standard molar free energy of the interaction into contributions of particular intermolecular contacts, and hence to elucidate stacking−hydrogen bonding cooperativity, and the two-step mechanism of cap−eIF4E recognition (3). The aim of the present report is to analyze the specific binding between eIF4E and a dinucleotide mRNA 5′ cap-analogue, 7-methylGpppG (Scheme 1), in terms of exact quantitative thermodynamic parameters determined independently from the van't Hoff equation and isothermal titration calorimetry (ITC). Such quantitative data are of primary importance for the rational design of new cap-analogues of potential therapeutic activity since the high eIF4E cellular level is relevant to malignancy and apoptosis (8).

Binding studies on specific complexes involving proteins, nucleic acids, and small ligands have proven to be very useful to investigate the stabilization energy and the influence of

* Author to whom correspondence should be addressed at the Department of Biophysics, Institute of Experimental Physics, Warsaw University, 93 Zwirki & Wigury St., 02-089 Warszawa, Poland. E-mail: stolarsk@biogeo.uw.edu.pl; Tel: +48 22 55 40 714; Fax: +48 22 55 40 001.

‡ Warsaw University.
§ McGill University.

[1] Abbreviations: eIF4E, eukaryotic initiation factor 4E; 7-methyl-GpppG, P^1-7-methylguanosine-5′ P^3-guanosine-5′ triphosphate; 4E-BP, 4E-binding protein; Hepes, *N*-(2-hydroxyethyl)piperazine-*N*′-2-ethanesulfonic acid; DTT, dithiothreitol; EDTA, disodium ethylenediaminetetraacetate.

Scheme 1:   Chemical Structure of 7-MethylGpppG[a]
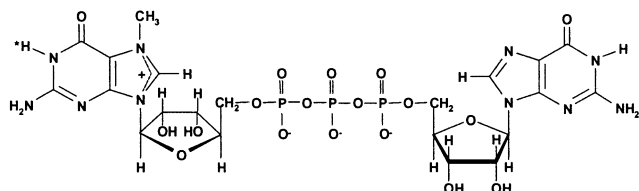
[a] The N(1)−H proton of 7-methylguanosine which partially dissociates at pH 7.2 [pK_a = 7.35 ± 0.05 (28)] is marked with an asterisk.

solvent on complex formation, e.g., polyelectrolytic effect, water exchange between the macromolecules and the solvent (9−12), and linked protonation equilibria (13, 14). The majority of reported studies show that the intermolecular association is accompanied by a negative change of the molar standard heat capacity at constant pressure (15, 16), what is mainly attributed to burial of the solvent accessible-hydrophobic molecular surface upon complex formation (17, 18). Considering that salt bridges, cation−π stacking, and hydrogen bonds play a dominant role in mRNA 5′ cap−eIF4E binding (2), this molecular system is significantly distinct from the hydrophobic ones which are usually a focus of the thermodynamic studies. The cap−eIF4E binding is also accompanied by other processes, i.e., the conformational change of the protein and the solvent effects, like additional hydration of the complex and proton uptake (3). Indications of the latter arose from the pH-dependence of the cap−eIF4E affinity. Herein we report a quantitative confirmation of the ligand protonation. Together, the present data contribute to a more profound understanding of eukaryotic translation initiation on the molecular level.

MATERIALS AND METHODS

7-MethylGpppG and eIF4E Preparations. Synthesis and purification of 7-methylGpppG were described elsewhere (19). The concentration was calculated from a weighted amount (±5%) and confirmed spectrophotometrically (6). Murine eukaryotic initiation factor eIF4E (residues 28−217) was expressed in *E. coli* (2, 20), purified from inclusion body pellets, and refolded by one-step dialysis from 6 M guanidinium hydrochloride followed by cation exchange chromatography on a 5 mL HiTrap SP column (Pharmacia, Sweden), without any contact with cap-analogues at any stage of purification. All chemicals were analytical grade, purchased from Sigma-Aldrich, Merck, or Carl Roth (Germany).

Spectroscopic Measurements and Data Analysis. Association constants were determined by intrinsic protein fluorescence quenching, as described previously (3, 21). The absorption and emission spectra were recorded on Lambda 20 UV/VIS and LS-50B instruments (Perkin-Elmer), respectively, in quartz semi-micro cuvettes (Hellma, Germany), thermostated within ±0.2 K. The temperature was controlled with a thermocouple inside the cuvette. The steady-state experiments were performed by a time-synchronized titration method (3). The fluorescence intensity, corrected for the *inner filter* effect (22), was monitored at a single wavelength, with an integration time of 30 s and a gap of 30 s for adding the cap-analogue, with magnetic stirring. During the gap, the UV xenon flash lamp was switched off to avoid photobleaching of the sample. The excitation wavelength of

280 nm (slit 2.5 nm, auto cutoff filter) and the emission wavelength of 335 nm (slit 2.5−4 nm, 290 nm cutoff filter) were applied, with a correction for the photomultiplier sensitivity.

Binding studies were carried out in 50 mM Hepes/KOH, 100 mM KCl, 1 mM DTT, 0.5 mM EDTA, at pH 7.20 ± 0.02, adjusted for each temperature on a Φ300 pH-meter (Beckman) assuming dpH/dT = −0.014 K^{-1} for Hepes. Each run consisted of more than 30 data points, with 1 μL aliquots of increasing 7-methylGpppG concentration (1 μM to 5 mM) added to 1400 μL of eIF4E solution. Dilution did not exceed 2.5%. The emission of free cap-analogues was explicitly included in the analysis. Runs were repeated several times for eIF4E at concentrations of 0.01−0.5 μM. Protein solution was filtered through Ultrafree-0.5 mL Biomax 100 kDa NMWL (Millipore). The total concentration of eIF4E was estimated from absorption, and the amount of the active protein was exactly fitted as a free parameter of the equilibrium equation (3, 21). The theoretical curve for the fluorescence intensity (F) as a function of the total ligand concentration ([L]) was fitted to the experimental data points by means of a nonlinear, least-squares method, using ORIGIN 6.0 (Microcal Software) according to the equation:

$$F = F(0) - [cx] \cdot (\Delta\phi + \phi_{\text{lig,free}}) + [L] \cdot \phi_{\text{lig,free}} \quad (1)$$

where the equilibrium concentration of the complex [cx] is given by

$$[cx] = \frac{[L] + [P_{\text{act}}]}{2} + \frac{1 - \sqrt{(K_{\text{as}} \cdot ([L] - [P_{\text{act}}]) + 1)^2 + 4K_{\text{as}} \cdot [P_{\text{act}}]}}{2 \cdot K_{\text{as}}} \quad (2)$$

The fitted parameters were as follows: K_{as}, the association constant, [P_{act}], the concentration of the active protein; $\Delta\phi = \phi_{\text{Pact}} - \phi_{\text{cx}}$, the difference between the fluorescence efficiencies of the apo-protein and the complex; $\phi_{\text{lig,free}}$, the fluorescence efficiency of the free cap-analogue in the solution; and $F(0)$, the initial fluorescence intensity. Total quenching was calculated as

$$Q = [P_{\text{act}}] \cdot \Delta\phi \quad (3)$$

For determination of the active protein fraction in the samples studied by ITC, the cap-analogue of the highest association constant for eIF4E, i.e., 7-methylGTP (3), was used, since this K_{as} ensures the optimal quotient of K_{as}/[P_{act}]. Such a quotient determines the suitable curvature of eq 1 in the range where the total ligand concentration is close to the active protein concentration:

$$\left| \frac{\partial^2 F}{\partial [L]^2} \right|_{[L]=[Pact]} \sim \sqrt{\frac{K_{\text{as}}}{P_{\text{act}}}}$$

which is required for the accurate fitting of [P_{act}].

The molar heat capacity change (ΔC_p°) and the characteristic temperatures (T_S where $\Delta S^{\circ} = 0$, and T_H where $\Delta H_{\text{vH}}^{\circ} = 0$, index "°" refers to the pseudostandard state at concentrations of 1 mol/L, i.e., unit molarity) were obtained from the nonlinear van't Hoff equation as free parameters

of the fitting (23−25):

$$\ln K_{as} = \frac{\Delta C_p^\circ}{R}\left[\frac{T_H}{T} - \ln\left(\frac{T_S}{T}\right) - 1\right] \quad (4)$$

ΔG°, ΔS°, and the van't Hoff enthalpy change, ΔH_{vH}°, were calculated as

$$\Delta G^\circ = -RT \ln K_{as} \quad (5)$$

$$\Delta S^\circ = \Delta C_p^\circ \ln\left(\frac{T}{T_S}\right) \quad (6)$$

$$\Delta H_{vH}^\circ = \Delta C_p^\circ(T - T_H) \quad (7)$$

Discrimination between the linear model ($\ln K_{as} = \Delta S^\circ/R - \Delta H_{vH}^\circ/RT$, where ΔH_{vH}°, $\Delta S^\circ = const$) and the nonlinear model (eq 4) was based of the Snedecor's F-test and R^2 value (26).

Calorimetric Measurements. ITC experiments were run on an OMEGA Ultrasensitive Titration Calorimeter (Micro-Cal), calibrated by 18-crown-6 titration with $BaCl_2$. Suitable buffers (50 mM Hepes/KOH, 100 mM KCl, 1 mM EDTA) were prepared to keep pH 7.20 ± 0.02 at 288.1, 293.1, 298.4, and 303.2 K. The protein sample buffer was exchanged by 4-fold centrifugation on 5 kDa Centricon filters (Millipore). After the last centrifugation, the flow-through buffer was collected to dissolve 7-methylGpppG and to control the ligand dilution. The concentration of the injected ligand was 1.00 ± 0.07 mM in each case. Samples were degassed, and then filtered through a 0.22 μm filter (Millipore) directly before use. The main part of each protein solution was used for ITC and the remaining part for the control fluorescence titration. This ensured consistency for all the measurements. The active protein concentrations at four temperatures were 8.97, 7.42, 3.61, and 5.35 μM, respectively.

Low solubility of eIF4E (28−217) hampered direct and precise determination of K_{as} by the ITC measurements. The very first injection of 7-methylGpppG into the eIF4E solution results in ~35 μJ of the evolved heat, so at the verge of the instrument sensitivity, ~40 μJ (recommended in the Micro-Cal OMEGA manual). The subsequent heat signals decrease with the course of the titration due to the negative value of ΔH°, thus becoming indiscernible from the noise. However, it was possible to determine the calorimetric enthalpies by a modified "single injection" method, with slow stirring at 240 rpm to avoid protein precipitation. The ligand solution was injected into the calorimetric cell (1386 μL volume) filled with eIF4E solution, and next the remaining 7-methylGpppG solution was injected into the buffer to measure the heat of dilution. Each experiment consisted of the main 40 μL injection, preceded by two 1 μL injections to calculate the correction for the initial outflow from the syringe, and followed by two 4 μL injections to check the protein saturation with the ligand. It was therefore possible to determine the total emitted heat in the most reliable way. After integration of all signals, the corresponding values from both series were subtracted from each other to yield the total calorimetric enthalpy ΔH_{cal}°. Calorimetric ΔC_p° values were calculated as slopes of the linear temperature-dependence of the enthalpies: ΔH_{cal}°, ΔH_{ion}°, $\Delta H_{cal-ion}^\circ = \Delta H_{cal}^\circ - \Delta H_{ion}^\circ$, and ΔH_0° (see below).

Buffer ionization heats (ΔH_{ion}°) at pH 7.2 were calculated as

$$\Delta H_{ion}^\circ = \frac{10^{-pK_a}}{10^{-pK_a} + 10^{-pH}}\cdot\Delta H_{H-diss}^\circ \quad (8)$$

from the proton ionization heat for Hepes, $\Delta H_{H-diss}^\circ = +20.95$ kJ·mol^{-1} at 298.2 K, and the temperature dependence of ΔH_{H-diss}° estimated as $\delta\Delta H_{H-diss}^\circ/\delta T = +0.0648$ kJ·mol^{-1}·K^{-1} (27), and p$K_a = 7.35 \pm 0.05$ for 7-methyl-GpppG (28). The pK_a changes were negligible over the temperature range used. The actual number of protons involved in the binding could be determined by measuring calorimetrically the enthalpy changes in buffers of different ionization heats in a more exhaustive way. However, the data derived from the measurements in Hepes were sufficient to verify our previous spectroscopic results (3) concerning the ionic state of the ligand, and each single ITC experiment would require a huge amount of the protein, more than that for 200 fluorescence titrations.

Coupling between the Binding and Conformational Transition of the Ligand. Thermodynamic parameters describing intramolecular base stacking of dinucleotide cap-analogues in the cationic form, i.e., entropy ($_1\Delta S^\circ$) and enthalpy ($_1\Delta H^\circ$) changes (29), were used for calculating the following quantities at four temperatures: stacking/unstacking equilibrium constants ($_1K$); contributions to enthalpy (ΔH_{sst}°), entropy (ΔS_{sst}°), and heat capacity ($\Delta C_{p_{sst}}^\circ$) changes, resulting from an induced shift in the self-stacking equilibrium; and intrinsic enthalpy (ΔH_0°) and entropy (ΔS_0°) changes of 7-methylGpppG−eIF4E binding (13):

$$_1K = \exp\left(\frac{_1\Delta S^\circ}{R} - \frac{_1\Delta H^\circ}{RT}\right) \quad (9)$$

$$\Delta H_{sst}^\circ = -\frac{_1\Delta H^\circ\cdot_1K}{1 + _1K} \quad (10)$$

$$\Delta S_{sst}^\circ = -R \ln(1 + _1K) - \frac{_1\Delta H^\circ\cdot_1K}{T(1 + _1K)} \quad (11)$$

$$\Delta C_{p_{sst}}^\circ = -\frac{(_1\Delta H^\circ)^2\cdot_1K}{RT^2(1 + _1K)^2} \quad (12)$$

$$\Delta H_0^\circ = \Delta H_{cal-ion}^\circ - \Delta H_{sst}^\circ \quad (13)$$

$$\Delta S_0^\circ = \Delta S^\circ - \Delta S_{sst}^\circ \quad (14)$$

Errors of all reported values (one standard deviation) were calculated according to the propagation rules on the basis of experimental and numerical uncertainty resulting from the fitting (30).

RESULTS AND DISCUSSION

Thermodynamics of eIF4E Association with 7-Methyl-GpppG. Interaction between the 7-methylguanine moiety and eIF4E results in quenching of the intrinsic protein fluorescence (31). Typical titrations of eIF4E with 7-methylGpppG at four selected temperatures are presented in Figure 1. The equilibrium association constants (K_{as}) and the corresponding standard molar free energies of the complex formation (ΔG°)
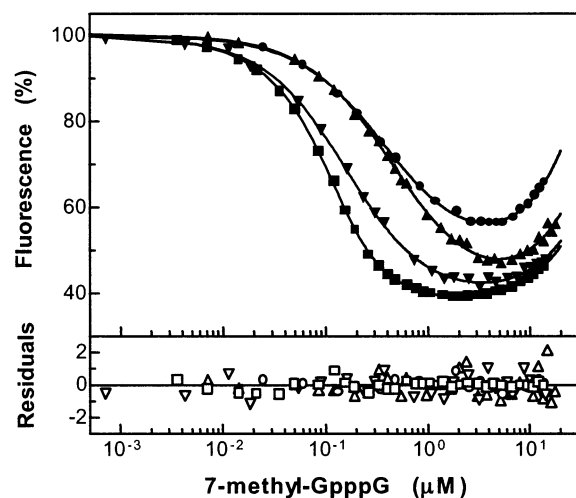
FIGURE 1: Quenching of eIF4E intrinsic fluorescence upon titration with 7-methylGpppG at different temperatures: (●) 312.6, (▲) 304.9, (▼) 293.2, (■) 288.2 K, and fitting residuals (eqs 1 and 2). Increasing fluorescence intensity at higher concentration of 7-methylGpppG originates from the free ligand in solution. Titrations were performed in 50 mM Hepes/KOH (pH 7.2), 100 mM KCl, 1 mM DTT, 0.5 mM EDTA.
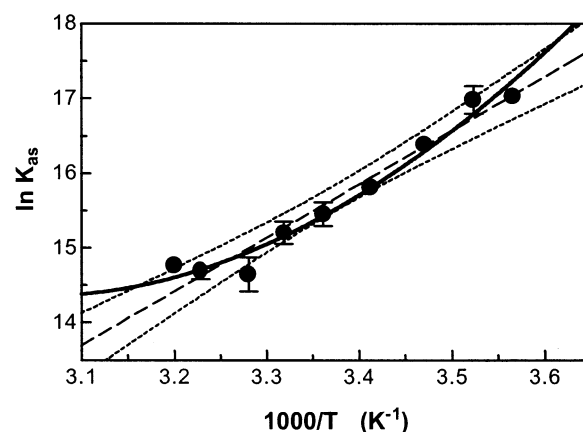

FIGURE 2: van't Hoff plot for the specific interaction of 7-methylGpppG with eIF4E. Nonlinear regression (solid thick line) is obtained by fitting eq 4 to experimental data points (Table 1). Linear regression (broken thin line) with 95% confidence interval is shown for comparison.

Table 1: Association Constants (K_{as}) and Standard Molar Free Energies ($\Delta G°$) for Binding of 7-MethylGpppG to eIF4E

temperature (K)	$K_{as} (\mu M^{-1})$	$\Delta G° (kJ \cdot mol^{-1})$
280.6	24.9 ± 1.1	−39.73 ± 0.10
283.9	23.7 ± 4.3	−40.08 ± 0.44
288.2	12.9 ± 1.2	−39.23 ± 0.22
293.2[a]	7.39 ± 0.46	−38.55 ± 0.15
297.6	5.13 ± 0.81	−38.22 ± 0.38
301.4	4.01 ± 0.61	−38.10 ± 0.37
304.9	2.29 ± 0.52	−37.12 ± 0.55
309.8	2.41 ± 0.27	−37.84 ± 0.27
312.6	2.56 ± 0.22	−38.35 ± 0.21

[a] Data from (*3*).

are gathered in Table 1. The association constant at 293.2 K ($K_{as} = 7.39 ± 0.46 \mu M^{-1}$) is very close to that for full-length human eIF4E [$9.6 ± 0.8 \mu M^{-1}$ (*21*)] under the same experimental conditions. Recently, the human eIF4E−7-methylGpppG binding affinity was fluorometrically studied in the context of cell growth suppression, and the association constant of $0.83 ± 0.14 \mu M^{-1}$ was reported (296.2 K, pH 7.5, 300 mM KCl) (*32*). The corresponding K_{as} value reported herein for truncated murine eIF4E (residues 28−217) is 5.13 ± 0.81 μM^{-1} (297.6 K, pH 7.2, 100 mM KCl). These results are in an excellent agreement, since elevation of KCl concentrations from 100 to 300 mM causes a significant, ∼6-fold decrease of the association constant due to screening of the electrostatic attraction between the basic amino acids in the cap-binding site of eIF4E and the phosphate chain of 7-methylGpppG (*3*).

The van't Hoff dependence of ln K_{as} vs $1/T$ exhibits nonlinear behavior (Figure 2), characterized by a large, positive value of the standard heat capacity change: $\Delta C_p° = +1.92 ± 0.93$ kJ·mol^{-1}·K^{-1}, with the critical temperatures $T_S = 307.4 ± 6.0$ K and $T_H = 327.1 ± 15.2$ K. The results derived from the nonlinear fit are statistically better than those derived from the linear one, on the significance level of $P = 0.08$ from the Snedecore's F-test.

Molecular associations involving proteins, like specific protein−DNA interactions, formation of enzyme−ligand
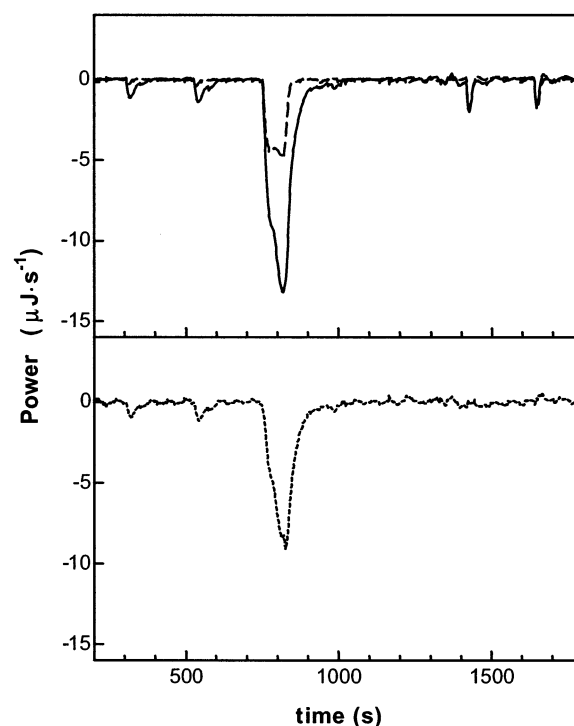

FIGURE 3: ITC curves for modified "single injection" experiment at 288.1 K. 7-MethylGpppG solution was injected into eIF4E solution (solid line) and into buffer (50 mM Hepes/KOH, pH 7.2, 100 mM KCl, 1 mM EDTA) (broken line). The main injection (volume 40 μL) was preceded by two 1 μL injections, providing a correction for the instrumental artifacts, and followed by two 4 μL injections to check the saturation of eIF4E. The resultant heat excess of 7-methylGpppG binding to eIF4E is shown in the bottom panel (dotted line).

complexes, and antigene−antibody recognition, are usually characterized by substantial, negative values of the standard heat capacity change $\Delta C_p°$ (*15*, *18*). Hence, to confirm the validity of our distinct spectroscopic results, the direct calorimetric measurements of the standard enthalpy change $\Delta H_{cal}°$ at four different temperatures were carried out (Figure 3). To control the activity of eIF4E, which is a nonenzymatic, highly unstable protein [instability index = 47.41 (*33*) for murine eIF4E (28−217)], concurrent fluorometric titrations were run with use of the same protein
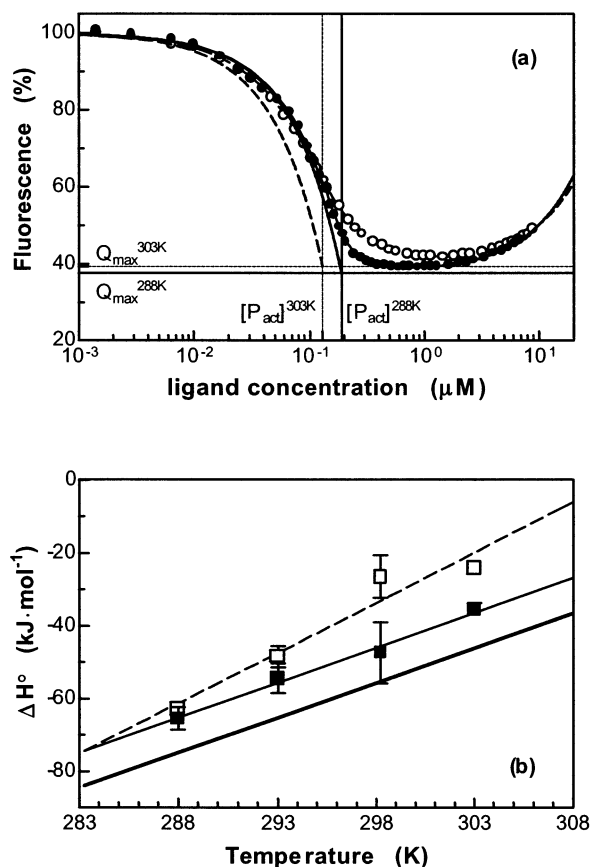
FIGURE 4: (a) Determination of protein active fractions at 303.2 K (○, broken lines) and 288.1 K (●, solid lines). Titration curves determine both K_{as} and $[P_{act}]$ as free parameters of the fitting (eqs 1 and 2). $[P_{act}]$ is graphically represented by the point where the curve for hypothetical infinite K_{as} would attain maximal quenching, Q_{max} (eq 3). (b) Total calorimetric enthalpies corrected for ligand dilution, assuming 100% protein activity (□, broken thin line), and those corrected also for active protein concentration, as determined from fluorometric titration (■, solid thin line). Temperature dependence of the van't Hoff enthalpy is shown for comparison (solid thick line).

samples as for ITC, incubated at a given temperature for the same time as for the calorimetric measurements. The precise time-synchronized measurements of the protein intrinsic fluorescence quenching enabled us to determine the concentrations of active protein ($[P_{act}]$) at each temperature (Figure 4a). The enthalpy estimates for the assumed 100% protein activity, and those corrected for the active protein concentration determined from fluorometric titrations, are shown in comparison with the van't Hoff enthalpy change (Figure 4b). The calorimetric enthalpies yield a slope ΔC_p° = +1.966 ± 0.061 kJ·mol^{-1}·K^{-1}, what confirms the result of the van't Hoff analysis.

Protonation Equilibria. A systematic positive shift of the calorimetric enthalpies (ΔH_{cal}°) in comparison with their van't Hoff counterparts (ΔH_{vH}°) appears from the data (Figure 4b, Table 2). Although the numerical uncertainty of ΔH_{vH}° is about ±30 kJ·mol^{-1}, the average value of the difference between ΔH_{cal}° and ΔH_{vH}° of about +9.7 kJ·mol^{-1} seems to be well specified. Differences between the calorimetric and the van't Hoff enthalpy estimates were the subject of empirical and theoretical analyses for various association processes (*34–39*). The observed discrepancies were ascribed to contributions of usually unknown molecular transitions

or coupled processes, other than the net complex formation, to ΔH_{cal}°, and/or erroneous apparent values of ΔH_{vH}° and ΔC_p°, arising from the experimental noise. In the case of cap−eIF4E binding, the latter obscuring effect is eliminated, as testified by the accordance of the van't Hoff and calorimetric ΔC_p° values. This approximately constant difference can be analyzed in terms of the protonation equilibria (*40*). 7-MethylGpppG exists as a mixture of cationic (58%) and zwitterionic (42%) forms at pH 7.2 [pK_a = 7.35 ± 0.05 for the N(1)−H proton of the 7-methylguanine moiety (*28*), Scheme 1]. Several contradictory conclusions were reported regarding the ionic state of the mRNA 5′ cap that binds to eIF4E most tightly. Initially, the zwitterionic form of 7-methylguanine was postulated to interact with eIF4E (*4*, *5*). In contrast, the crystallographic and NMR structures revealed the spatial distances suitable for formation of a hydrogen bond between Glu103 and N(1)−H of 7-methyl-guanine (*2*, *3*, *41*, *42*), pointing to the cationic form of 7-methylguanine. This hydrogen bond is also present in the ternary 7-methylGDP−eIF4E−eIF4GII peptide complex at pH 8.5 (*43*). However, the N(1)−H proton has not been directly observed by NMR (*41*). Recent spectroscopic binding studies as a function of pH showed the upward shift of the pK_a of N(1)−H inside the eIF4E binding site, suggesting that the tightest binding is accomplished through the cationic form of 7-methylguanosine (*3*). The eIF4E−cap association that is accompanied by the putative partial protonation of the ligand must be equilibrated by additional deprotonation of the buffer to keep the cation−zwitterion equilibrium of the free ligand at constant pH. As shown in Table 2, the contributions of the Hepes ionization heats (ΔH_{ion}°) to the total reaction heats are in good agreement with the difference between ΔH_{cal}° and ΔH_{vH}°. This demonstrates the linkage between 7-methylGpppG−eIF4E binding and concomitant protonation of the residue which has pK_a = 7.35 in the unbound state. Taking into account the net calorimetric enthalpy changes related to cap binding to eIF4E, $\Delta H_{cal-ion}^\circ = \Delta H_{cal}^\circ - \Delta H_{ion}^\circ$ (Figure 5, Table 2), the calorimetric heat capacity change is ΔC_p° = +1.941 ± 0.059 kJ·mol^{-1}·K^{-1}.

The coupling of the binding process with the acidic−basic equilibrium of the ligand is nonmandatory (*13*), since the zwitterionic form of 7-methylGpppG is able to bind to the protein via weaker interactions of the 7-methylG moiety and almost unchanged interactions of the phosphate chain (*3*). It was shown that the protein-induced shift in the two-state transition of the ligand can contribute to the observed heat capacity change (*13*). This contribution may be either positive or negative, depending on the unknown values of the intrinsic enthalpy changes and equilibrium constants that describe binding of the cationic and the zwitterionic forms of 7-methylGpppG to eIF4E independently.

Conformational Equilibrium of the Ligand. The eIF4E−cap binding process is also directly coupled with intramolecular self-stacking of the dinucleotide cap-analogues. The coupled processes provide for additional enthalpic (ΔH_{sst}°) and entropic (ΔS_{sst}°) contributions, and an apparent molar heat capacity change (ΔC_{psst}°), resulting from an induced shift in the conformational equilibrium of the ligand upon binding to the protein (*13*). The known thermodynamic parameters for the self-stacking of the cationic form of 7-methylGpppG [$_1\Delta H^\circ$ = −15.2 ± 0.5 kJ·mol^{-1}, $_1\Delta S^\circ$ =

Table 2: Thermodynamic Parameters for Binding of 7-MethylGpppG to eIF4E

	temperature (K)				heat capacity change, ΔC_p° (kJ·mol^{-1}K^{-1})
	288.1	293.1	298.4	303.2	
	Enthalpy Change (kJ·mol^{-1})				
ΔH_{cal}° [a]	-65.5 ± 3.2	-54.4 ± 4.0	-47.3 ± 8.4	-35.5 ± 1.7	$+1.966 \pm 0.061$ [i]
ΔH_{ion}° [b]	$+8.53$	$+8.66$	$+8.81$	$+8.94$	$+0.0273 \pm 0.0003$ [i]
$\Delta H_{cal-ion}^{\circ}$ [c]	-74.0 ± 3.2	-63.1 ± 4.0	-56.1 ± 8.4	-44.4 ± 1.7	$+1.941 \pm 0.059$ [i]
ΔH_{vH}° [d]	-75 ± 36	-65 ± 31	-56 ± 26	-46 ± 22	$+1.92 \pm 0.93$ [j]
ΔH_{sst}° [e]	$+10.13 \pm 1.13$	$+9.76 \pm 1.15$	$+9.37 \pm 1.17$	$+9.01 \pm 1.18$	-0.0741 ± 0.0002 [i]
ΔH_0° [f]	-84.1 ± 3.4	-72.9 ± 4.2	-65.47 ± 8.5	-53.4 ± 2.1	$+2.014 \pm 0.064$ [i]
	Entropy Change (J·mol^{-1}·K^{-1})				
ΔS° [g]	-124 ± 71	-91 ± 58	-57 ± 47	-26 ± 40	
ΔS_{sst}° [e]	$+26.0 \pm 2.2$	$+24.8 \pm 2.1$	$+23.4 \pm 2.0$	$+22.3 \pm 1.9$	
ΔS_0° [h]	-151 ± 71	-116 ± 58	-81 ± 47	-49 ± 40	

[a] Directly measured total enthalpy changes. [b] Buffer ionization heats at pH 7.2 (eq 8); estimated $\delta\Delta H_{ion}^{\circ} = \pm 0.09$. [c] Net calorimetric enthalpy changes, $\Delta H_{cal-ion}^{\circ} = \Delta H_{cal}^{\circ} - \Delta H_{ion}^{\circ}$. [d] van't Hoff enthalpy changes (eq 7). [e] Enthalpic and entropic contributions from an induced shift in the self-stacking equilibrium of 7-methylGpppG upon binding to eIF4E (eqs 10 and 11). [f] Intrinsic enthalpy changes of 7-methylGpppG−eIF4E binding (eq 13). [g] Apparent entropy changes (eq 6). [h] Intrinsic entropy changes of 7-methylGpppG−eIF4E binding (eq 14). [i] Calculated from linear temperature-dependence of corresponding ΔH_x°. [j] Calculated from nonlinear van't Hoff dependence (eq 4).
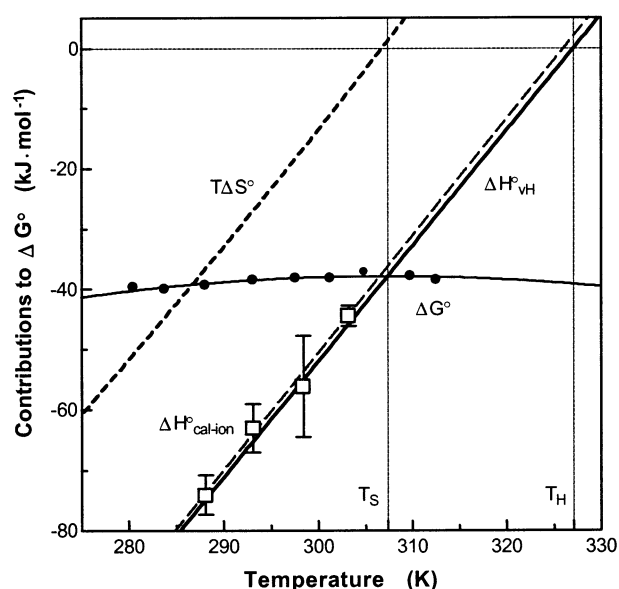

FIGURE 5: Enthalpy−entropy compensation that accompanies the binding of 7-methylGpppG to eIF4E. Theoretical fit (eq 5, solid thin line) to the binding free energies ΔG° (●), contributions of the entropy (eq 6, dotted thick line) and the van't Hoff enthalpy (eq 7, solid thick line) to ΔG°, as well as the calorimetric enthalpies corrected for ligand dilution, protein activity, and buffer ionization heat (□) with the linear regression (broken thin line) are plotted as a function of temperature. The binding is enthalpy-driven and entropy-opposed below $T_S = 307.4 \pm 6.0$ K, enthalpy- and entropy-driven between T_S and $T_H = 327.1 \pm 15.2$ K, and entropy-driven and enthalpy-opposed above T_H.

-47 ± 2 J·mol^{-1}·K^{-1} (*29*)] give a possibility to assess the influence of this coupled process on cap−eIF4E complex formation. As only the unstacked form is capable of penetrating the eIF4E cap-binding slot, the coupling should be regarded as a mandatory one. Both ΔH_{sst}° and ΔS_{sst}° are positive and relatively large (Table 2), which reduces the negative values of the intrinsic thermodynamic parameters, ΔH_0° by 12−17% and ΔS_0° even by 17−46%. This leads to the apparent less negative values of $\Delta H_{cal-ion}^{\circ}$ and ΔS_0°. While enthalpy and entropy changes of cap−eIF4E binding are profoundly affected by the coupling between binding and unstacking of 7-methylGpppG, the negative $\Delta C_{p_{sst}}^{\circ}$ contribution is small and almost constant [-74.4 ± 9.3, -74.3 ± 8.3, -73.8 ± 7.2, -73.0 ± 6.4

J·mol^{-1}·K^{-1} at 288.1 293.1, 298.4, 303.2 K, respectively (eq 12)]. Assuming constant temperature-dependence of ΔH_{sst}°, the average value of $\Delta C_{p_{sst}}^{\circ}$ is -74.1 ± 0.2 J·mol^{-1}·K^{-1} (Table 2), and shifts negligibly the heat capacity change of the overall cap−eIF4E association from the intrinsic value of $+2.014 \pm 0.064$ kJ·mol^{-1}·K^{-1} to the resultant value of $+1.941 \pm 0.059$ kJ·mol^{-1}·K^{-1} (Table 2). However, $\Delta C_{p_{sst}}^{\circ}$ is very close to a value found as a contribution due to the coupling of adenine base unstacking to binding between dA-(pA)$_{34}$ and the *E. coli* SSB protein, -62.8 ± 2.5 J·mol^{-1}·K^{-1} per one stack (*44*). This suggests that unstacking of the dinucleotide mRNA 5′ cap-analogue, i.e., between 7-methyl-guanosine and guanosine moieties linked via a 5′−5′ triphosphate bridge, can be energetically considered in a similar way as the oligodeoxyadenylate unstacking that accompanies specific binding of proteins to single-stranded DNA.

Molecular Interpretation of the Positive ΔC_p°. As a consequence of the large positive ΔC_p° value, strong enthalpy−entropy compensation for the eIF4E−7-methyl-GpppG association occurs, i.e., the values of both the linear ΔH_{vH}° term and the logarithmic $T\Delta S^{\circ}$ term increase with temperature, with nearly identical slopes (Figure 5). The binding is enthalpy-driven at temperatures below T_S (~307 K), while the entropy is unfavorable, confirming the importance of electrostatic stabilization of the complex (*3*). Then, the interaction changes its thermodynamic character to both enthalpy- and entropy-driven between T_S and T_H, and finally, above T_H the association becomes entropy-driven and enthalpy-opposed. Although the ΔG° function attains its maximum at T_S, the stabilization of the complex does not decrease rapidly but is still efficient ($\Delta G_{max}^{\circ} \sim -37.8$ kJ·mol^{-1}). The salient feature is that the eIF4E−7-methylGpppG interaction is both enthalpy- and entropy-favorable at biological temperatures (~310 K), and that the free energy of stabilization is relatively temperature-invariant over this range. This is of special biological importance, because the regulation of eIF4E and its inhibitory binding protein, 4E-BP1 (also known as PHAS-I, phosphorylated heat- and acid-stable protein regulated by insulin), is affected by heat shock which causes an increase of the association between eIF4E and 4E-BP1 (*45*). Increased binding of 4E-BP1 to eIF4E could interfere with the function of the active eIF4F

translation initiation complex (*46*) during heat shock (*47−50*). As mRNAs of heat shock proteins are relatively cap-independent (*51*, *52*), the enhanced inhibition of eIF4E by 4E-BP1 together with the temperature-invariant cap-binding affinity of eIF4E could provide a mechanism for the selective up-regulation of the synthesis of heat shock proteins.

Our results are contradictory to the first conclusions drawn from studies of 7-methylGTP and 7-methylGpppG binding to eIF4E from human erythrocytes (*5*). Although the human (*53*) and murine (*54*) proteins are almost identical [98% homology for the full-length proteins, and 100% for truncated (28−217) eIF4E], those results suggested that the eIF4E−cap binding was entropy-driven and enthalpy-opposed, with the constant thermodynamic parameters in the 278−308 K temperature range [$\Delta S° = +219 \pm 11$ J·mol^{-1}·K^{-1}, $\Delta H° = +33.9 \pm 1.7$ kJ·mol^{-1} for 7-methylGpppG (*5*)]. However, the human protein was purified by means of cap-affinity chromatography, what could result in up to 60% of the unremovable cap-analogue bound to eIF4E (*3*, *55*). This purification method yielded the apparent association constants up to 300-fold lower than those measured for eIF4E purified without contact with cap (*3*, *56*). Moreover, the decreasing temperature-dependence of the human eIF4E activity was not taken into account, and the authors reported the fluorescence intensity of eIF4E as invariant over the temperature range studied, which seems to be unlikely. Taken together, these main reasons could lead to misinterpretation of the experimental data.

Usually observed large, negative values of the standard heat capacity change are characteristic for specific hydrophobic binding between proteins and nucleic acids as well as for protein folding (*17*, *18*, *57*, *58*). The main negative contribution to $\Delta C_p°$ comes from the hydrophobic effect, i.e., the removal of nonpolar molecular surface from water upon complex formation. In contrary, the reduction of the polar surface area gives positive contribution to $\Delta C_p°$, although to less extent: 2.3-fold (*17*) or 1.7-fold (*59*), depending on the proposed model. Other contributions comprise changes in soft internal vibrational modes and temperature-dependent conformational changes and/or protein aggregation (*15*). A process of protein−ligand interaction characterized itself by $\Delta C_p° = 0$ can also give rise to nonzero, positive, or negative heat capacity change, due to coupling with other possible transitions (*13*): proton uptake or dissociation, binding of the second ligand, a conformational change of the protein and/or the ligand.

While the positive $\Delta C_p°$ relevant to the protein unfolding is a common observation, examples reported for intermolecular interactions are very rare, e.g., the formation of the phosphofructokinase tetramer (*60*), the interaction of the brain natriuretic peptide with heparin (*61*), cobalt hexamine, and spermidine binding to DNA (*62*). On the other hand, it was shown for the interaction of the c-Myb DNA-binding domain (R2R3) with its target DNA, that the heat capacity change can be strongly temperature- and ionic strength-dependent, leading even to sign inversion of $\Delta C_p°$ within some ranges of those parameters (*63*). In each case, Coulombic interactions were involved in the binding processes.

The kinetic studies of the eIF4E−cap interaction by means of stopped-flow fluorescence spectroscopy as well as Brownian molecular dynamics simulations (*7*) revealed the two-step character of complex formation. The first step is the diffusionally and electrostatically controlled encounter of the protein and the ligand, and the second step is the internal rearrangement of the encounter complex. Detailed analysis of the salt effect on the equilibrium association constants revealed that an uptake of roughly 65 water molecules to the first-layer hydration shell is necessary for complex formation (*3*). This large hydration effect is relevant to significant conformational change of the protein upon the second step of cap binding (*3*), and leads to an increase of the protein solvent-accessible surface area. Both the hydrophobic and polar residues can be exposed to water, but contribution of the latter to the $\Delta C_p°$ is smaller (*17*, *59*), and additionally can be canceled by the burial of the polar groups in the protein binding center.

Careful inspection of the crystallographic (*2*, *3*, *42*) and NMR (*41*) structural data shows that stabilization of the mRNA 5′ cap−eIF4E complexes is accomplished to a great extent by electrostatic interactions and partially complemented by the van der Waals and hydrophobic contacts. Many charged and uncharged polar groups are removed from water upon the association. The negatively charged 5′−5′ phosphate chain of 7-methylGpppG is a primary anchor to the positively charged Arg112, Lys162, Arg157, and Lys159 side-chains of eIF4E (*3*). This charge-to-charge anchoring makes it possible to form further specific contacts in the narrow binding slot: cation−π sandwich stacking of the 7-methylguanine moiety with Trp56 and Trp102, and three hydrogen bonds with Glu103 and Trp102. The cation−π stacking itself has also a great electrostatic component, resulting from the attraction between the cation and the quadrupole charge distribution of the aromatic ring, which dominates the polarizability and dispersive forces (*64−66*).

Both effects, the extensive hydration and presumably the burial of charged ligand and protein polar groups in the binding site, can make the $\Delta C_p°$ sign positive (*15*). Similarly, the positive $\Delta C_p°$ values, $+1.66 \pm 0.57$ to $+5.12 \pm 0.48$ kJ·mol^{-1}·K^{-1}, were unambiguously determined from the van't Hoff equation for several other cap-analogues of moderate affinity for eIF4E, i.e., 7-methylGpppp-(7-methylG), 7-methylGMP, 7-methylGpppC, N^2,N^2,7-trimethylGTP, at the significance level from 0.049 to less than 0.0001 in the Snedecor's F-test (Niedzwiecka, A., et al., in preparation). These $\Delta C_p°$ values correlate with the affinity of the cap-analogues for eIF4E: the stronger binding the less positive $\Delta C_p°$. The cap-analogues of the highest binding constants, e.g., 7-methylGTP (*3*), do not reveal any observable curvature of the van't Hoff plot. This is most probably due to tightening of the protein structure upon binding, that causes the conversion of some soft internal vibrational modes into stiffer ones, and yields the negative contribution to $\Delta C_p°$ (*15*). For the most specific cap-analogues, these two counteracting effects, i.e., the negative vibrational effect related to the specificity of binding and the unspecific positive surface effect, can make the $\Delta C_p°$ value too small to be discerned within the noise of the experimental data (*37*).

CONCLUSIONS

The spectroscopic and ITC studies reported herein bring us nearer to a well-embedded molecular model of the

translation initiation. It becomes clear that the general description of the cap−eIF4E association is complex due to strict synergy of dominating electrostatic and partially hydrophobic interactions in the binding site. Besides, it is thermodynamically coupled with other inter- and/or intramolecular processes: protonation and conformational transition of the cap, and the protein rearrangement accompanied by the water uptake. The induced shift in the self-stacking equilibrium of the dinucleotide cap-analogue gives a negligible negative contribution to the overall ΔC_p°. The exceptional, large positive standard heat capacity change ΔC_p° of the binding can be attributed mainly to the extensive additional hydration, and partially to the burial of the polar groups of the interacting molecules. The eIF4E−7-methylGpppG interaction reveals the enthalpy-driven character below 327 K and has the conducive entropy at temperatures above 307 K. As a consequence, the binding is both enthalpy- and entropy-driven over the range of biological temperatures, and the stability of the eIF4E−7-methylGpppG complex is almost temperature-independent. These properties make our molecular system unique in the thermodynamic sense, especially suitable for further development of quantitative interpretation of intermolecular recognition specificity.

ACKNOWLEDGMENT

REFERENCES

1. Sonenberg, N. (1988) *Prog. Nucleic Acid Res. Mol. Biol. 35*, 173−207.
2. Marcotrigiano, J., Gingras, A. C., Sonenberg, N., and Burley, S. K. (1997) *Cell 89*, 951−961.
3. Niedzwiecka, A., Marcotrigiano, J., Stepinski, J., Jankowska-Anyszka, M., Wyslouch-Cieszynska, A., Dadlez, M., Gingras, A. C., Mak, P., Darzynkiewicz, E., Sonenberg, N., Burley, S. K., and Stolarski, R. (2002) *J. Mol. Biol. 319*, 615−635.
4. Rhoads, R. E., Hellmann, G. M., Remy, P., and Ebel, J. P. (1983) *Biochemistry 22*, 6084−6088.
5. Carberry, S. E., Rhoads, R. E., and Goss, D. J. (1989) *Biochemistry 28*, 8078−8083.
6. Cai, A., Jankowska-Anyszka, M., Centers, A., Chlebicka, L., Stepinski, J., Stolarski, R., Darzynkiewicz, E., and Rhoads, R. E. (1999) *Biochemistry 38*, 8538−8547.
7. Blachut-Okrasinska, E., Bojarska, E., Niedzwiecka, A., Chlebicka, L., Darzynkiewicz, E., Stolarski, R., Stepinski, J., and Antosiewicz, J. M. (2000) *Eur. Biophys. J. 29*, 487−498.
8. Gingras, A. C., Raught, B., and Sonenberg, N. (1999) *Annu. Rev. Biochem. 68*, 913−963.
9. Record, M. T., Jr., Ha, J. H., and Fisher, M. A. (1991) *Methods Enzymol. 208*, 291−343.
10. Parsegian, V. A., Rand, R. P., and Rau, D. C. (1995) *Methods Enzymol. 259*, 43−94.
11. Chaires, J. B., Satyanarayana, S., Suh, D., Fokt, I., Przewloka, T., and Priebe, W. (1996) *Biochemistry 35*, 2047−2053.
12. Qu, X., and Chaires, J. B. (2001) *J. Am. Chem. Soc. 123*, 1−7.
13. Eftink, M. R., Anusiem, A. C., and Biltonen, R. L. (1983) *Biochemistry 22*, 3884−3896.
14. Baker, B. M., and Murphy, K. P. (1996) *Biophys. J. 71*, 2049−2055.
15. Sturtevant, J. M. (1977) *Proc. Natl. Acad. Sci. U.S.A. 74*, 2236−2240.
16. Patikoglou, G., and Burley, S. K. (1997) *Annu. Rev. Biophys. Biomol. Struct. 26*, 289−325.
17. Spolar, R. S., Livingstone, J. R., and Record, M. T., Jr. (1992) *Biochemistry 31*, 3947−3955.
18. Spolar, R. S., and Record, M. T., Jr. (1994) *Science 263*, 777−784.
19. Darzynkiewicz, E., Stepinski, J., Tahara, S. M., Stolarski, R., Ekiel, I., Haber, D., Neuvonen, K., Lehikoinen, P., Labadi, I., and Lonnberg, H. (1990) *Nucleosides Nucleotides 9*, 599−618.
20. Edery, I., Altmann, M., and Sonenberg, N. (1988) *Gene 74*, 517−525.
21. Niedzwiecka-Kornas, A., Chlebicka, L., Stepinski, J., Jankowska-Anyszka, M., Wieczorek, Z., Darzynkiewicz, E., Rhoads, R. E., and Stolarski, R. (1999) *Collect. Symp. Ser. 2*, 214−218.
22. Parker, C. A. (1968) *Photoluminescence of Solutions*, Elsevier Publishing Company, Amsterdam.
23. Baldwin, R. L. (1986) *Proc. Natl. Acad. Sci. U.S.A. 83*, 8069−8072.
24. Becktel, W. J., and Schellman, J. A. (1987) *Biopolymers 26*, 1859−1877.
25. Ha, J. H., Spolar, R. S., and Record, M. T., Jr. (1989) *J. Mol. Biol. 209*, 801−816.
26. Beyer, W. H. (1987) *CRC Standard mathematical tables*, CRC Press, Boca Raton, FL.
27. Christensen, J. J., Hansen, L. D., and Izatt, R. M. (1976) *Handbook of proton ionization heats and related thermodynamic quantities*, John Wiley & Sons, New York.
28. Wieczorek, Z., Stepinski, J., Jankowska, M., and Lonnberg, H. (1995) *J. Photochem. Photobiol. B 28*, 57−63.
29. Wieczorek, Z., Zdanowski, K., Chlebicka, L., Stepinski, J., Jankowska, M., Kierdaszuk, B., Temeriusz, A., Darzynkiewicz, E., and Stolarski, R. (1997) *Biochim. Biophys. Acta 1354*, 145−152.
30. Taylor, J. R. (1982) *An introduction to error analysis*, University Science Books, Mill Valley, CA.
31. McCubbin, W. D., Edery, I., Altmann, M., Sonenberg, N., and Kay, C. M. (1988) *J. Biol. Chem. 263*, 17663−17671.
32. Kentsis, A., Dwyer, E. C., Perez, J. M., Sharma, M., Chen, A., Pan, Z. Q., and Borden, K. L. (2001) *J. Mol. Biol. 312*, 609−623.
33. Guruprasad, K., Reddy, B. V., and Pandit, M. W. (1990) *Protein Eng. 4*, 155−161.
34. Naghibi, H., Tamura, A., and Sturtevant, J. M. (1995) *Proc. Natl. Acad. Sci. U.S.A. 92*, 5597−5599.
35. Liu, Y., and Sturtevant, J. M. (1995) *Protein Sci. 4*, 2559−2561.
36. Liu, Y., and Sturtevant, J. M. (1997) *Biophys. Chem. 64*, 121−126.
37. Chaires, J. B. (1997) *Biophys. Chem. 64*, 15−23.
38. Rouzina, I., and Bloomfield, V. A. (1999) *Biophys. J. 77*, 3242−3251.
39. Horn, J. R., Russell, D., Lewis, E. A., and Murphy, K. P. (2001) *Biochemistry 40*, 1774−1778.
40. Kavanoor, M., and Eftink, M. R. (1997) *Biophys. Chem. 66*, 43−55.
41. Matsuo, H., Li, H., McGuire, A. M., Fletcher, C. M., Gingras, A. C., Sonenberg, N., and Wagner, G. (1997) *Nat. Struct. Biol. 4*, 717−724.
42. Tomoo, K., Shen, X., Okabe, K., Nozoe, Y., Fukuhara, S., Morino, S., Ishida, T., Taniguchi, T., Hasegawa, H., Terashima, A., Sasaki, M., Katsuya, Y., Kitamura, K., Miyoshi, H., Ishikawa, M., and Miura, K. (2002) *Biochem. J. 362*, 539−544.
43. Marcotrigiano, J., Gingras, A. C., Sonenberg, N., and Burley, S. K. (1999) *Mol. Cell 3*, 707−716.
44. Kozlov, A. G., and Lohman, T. M. (1999) *Biochemistry 38*, 7388−7397.
45. Vries, R. G., Flynn, A., Patel, J. C., Wang, X., Denton, R. M., and Proud, C. G. (1997) *J. Biol. Chem. 272*, 32779−32784.
46. Sonenberg, N. (1996) in *Translational Control* (Hershey, J. W. B., Mathews, M. B., and Sonenberg, N., Eds.) pp 245−269, Cold Spring Harbor Laboratory, Cold Spring Harbor, NY.
47. Panniers, R., Stewart, E. B., Merrick, W. C., and Henshaw, E. C. (1985) *J. Biol. Chem. 260*, 9648−9653.
48. Duncan, R., Milburn, S. C., and Hershey, J. W. (1987) *J. Biol. Chem. 262*, 380−388.
49. Lamphear, B. J., and Panniers, R. (1991) *J. Biol. Chem. 266*, 2789−2794.
50. Morley, S. J., and Pain, V. M. (1995) *Biochem. J. 312* (Pt. 2), 627−635.
51. Sierra, J. M., and Zapata, J. M. (1994) *Mol. Biol. Rep. 19*, 211−220.
52. Rhoads, R. E., and Lamphear, B. J. (1995) *Curr. Top. Microbiol. Immunol. 203*, 131−153.

53. Rychlik, W., Domier, L. L., Gardner, P. R., Hellmann, G. M., and Rhoads, R. E. (1987) *Proc. Natl. Acad. Sci. U.S.A. 84*, 945−949.

54. Altmann, M., Krieger, M., and Trachsel, H. (1989) *Nucleic Acids Res. 17*, 7520.

55. Shibata, S., Morino, S., Tomoo, K., In, Y., and Ishida, T. (1998) *Biochem. Biophys. Res. Commun. 247*, 213-216.

56. Wieczorek, Z., Niedzwiecka-Kornas, A., Chlebicka, L., Jankowska, M., Kiraga, K., Stepinski, J., Dadlez, M., Drabent, R., Darzynkiewicz, E., and Stolarski, R. (1999) *Z. Naturforsch., C: Biosci. 54*, 278−284.

57. Murphy, K. P., Privalov, P. L., and Gill, S. J. (1990) *Science 247*, 559−561.

58. Gomez, J., Hilser, V. J., Xie, D., and Freire, E. (1995) *Proteins: Struct., Funct., Genet. 22*, 404−412.

59. Murphy, K. P., Bhakuni, V., Xie, D., and Freire, E. (1992) *J. Mol. Biol. 227*, 293−306.

60. Luther, M. A., Cai, G. Z., and Lee, J. C. (1986) *Biochemistry 25*, 7931−7937.

61. Hileman, R. E., Jennings, R. N., and Linhardt, R. J. (1998) *Biochemistry 37*, 15231−15237.

62. Matulis, D., Rouzina, I., and Bloomfield, V. A. (2000) *J. Mol. Biol. 296*, 1053−1063.

63. Oda, M., Furukawa, K., Ogata, K., Sarai, A., and Nakamura, H. (1998) *J. Mol. Biol. 276*, 571−590.

64. Dougherty, D. A. (1996) *Science 271*, 163−168.

65. Mecozzi, S., West, A. P., and Dougherty, D. A. (1996) *J. Am. Chem. Soc. 118*, 2307−2308.

66. Mecozzi, S., West, A. P., Jr., and Dougherty, D. A. (1996) *Proc. Natl. Acad. Sci. U.S.A. 93*, 10566−10571.